Hindawi
Journal of Applied Mathematics
Volume 2019, Article ID 7463167, 9 pages
https://doi.org/10.1155/2019/7463167

Research Article

Modeling the Effects of Vaccination and Treatment on Tuberculosis Transmission Dynamics

Ashenafi Kelemu Mengistu and Peter J. Witbooi

Department of Mathematics and Applied Mathematics, University of the Western Cape, Private Bag X17, Bellville 7535, South Africa

Correspondence should be addressed to Peter J. Witbooi; pwitbooi@uwc.ac.za

Received 18 June 2019; Revised 31 August 2019; Accepted 1 October 2019; Published 23 December 2019

Academic Editor: Ali R. Ashrafi

In this study, we develop and analyze a deterministic mathematical model for tuberculosis (TB) transmission dynamics. The model includes vaccination for newborns and treatment for both high-risk latent and active TB patients. The stability of disease-free equilibrium point is discussed in detail. In the numerical simulation, the model parameters are estimated using reported TB incidence data in Ethiopia from the years 2003 to 2017, and $\mathscr{R}_0$ is calculated as $\mathscr{R}_0 \approx 2.13$. Finally, the sensitivity indices of $\mathscr{R}_0$ with respect to the model parameters are performed, and their corresponding graphical results are presented. Our results quantify the positive influence of vaccination and the treatment for high-risk latent and active TB patients on the control of tuberculosis.

1. Introduction

Tuberculosis (TB) is an airborne and highly infectious disease caused by *Mycobacterium tuberculosis*. A susceptible individual is infected with the bacteria when he or she inhales the TB germs, which are released into the air when infected individuals cough, sneeze, spit or talk [1]. The fight against TB involves vaccination with Bacillus Calmette-Guérin (BCG), screening of those at high risk, early detection, and treatment of cases [2]. In most TB endemic countries, BCG vaccination is recommended for tuberculosis prevention and is usually administered shortly after birth to prevent TB in infants [3, 4].

Globally, tuberculosis remains a major global health problem, and it is one of the top 10 causes of death and the leading cause of a single infectious agent (above HIV/AIDS). In 2017, an estimated 10 million people developed TB, and 1.3 million died from the disease (including 300,000 deaths among HIV-positive people) [5]. In Ethiopia, TB is still a serious public health challenge and one of the leading causes of morbidity and mortality [6]. According to the WHO report, Ethiopia is one of the 30 high-burden countries, and there were an estimated 172,000 (164 per 100,000 populations) incident cases of TB in 2017. According to the same report, there were an estimated 25,000 deaths (24 per 100,000) due to TB, excluding HIV related deaths.

Mathematical models and computer simulations are inexpensive, easy to manage, relatively fast, and quite productive experimental tools. They have been widely used to examine, explain, and predict the dynamics of infectious disease transmission. Starting from the first mathematical model for TB by Waaler et al. [7], different mathematical models for tuberculosis have been formulated, analyzed, and utilized. These models apply to different types of populations such as a city or country, a school, prison, or refugee camp, see for instance, [8, 9] Also, different models would focus on various factors such as progression rate, treatment, vaccination, immigration, etc. see [10–12].

For many years mathematical models have been applied to study the transmission dynamics of TB. For example, Zhao et al. [13] investigated the role of age on the transmission of TB in Mainland China and found that the BCG vaccine is useful only for younger people. They also recommended that the DOTS program should be more focused on the senior-aged group, and more attention should be given to people with latent TB in the middle-aged group. Choi et al. [14] introduced three control mechanisms: distancing, case finding, and case holding into the SEIL model in South Korea. They showed that distancing control is the most effective prevention mechanism of all. On the other hand, Moualeu et al. [15] developed a model for the transmission dynamics of TB and applied to the data for Cameroon. They identified that the combined effort that is education and

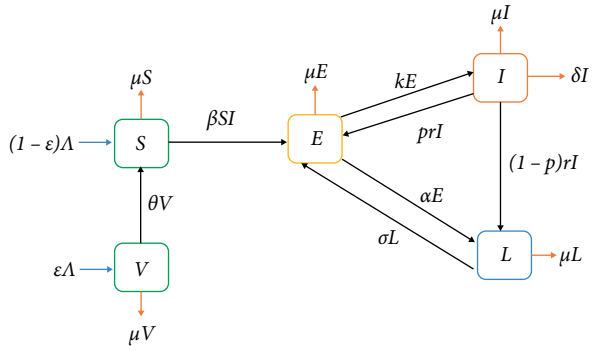

Figure 1: Flow diagram of the TB transmission model.

chemoprophylaxis might lead to a reduction of 80% in the number of infected people in 10 years. Kim et al. [16] developed a mathematical model for TB and fitted to the Philippine data. Their result showed that applying a combination of distancing and case finding control strategies has significant potential for curtailing the spread of TB in the Philippines. Therefore the transmission dynamics of TB by mathematical models are important for proposing the best mechanisms to control the spread of TB. The purpose of this study is to develop a suitable TB dynamics model and calibrating it for Ethiopia.

2. Materials and Methods

2.1. Model Formulation. The model that we present in this paper is the modification of the models in [14, 16] by including TB vaccination for newborns. The homogeneously mixing total population at time t, of size $N(t)$, is divided into five subclasses: susceptible $S(t)$, Vaccinated $V(t)$), high-risk latently infected, $E(t)$, Infectious (or active TB) $I(t)$, and low-risk latent $L(t)$.

We assume that the recruitment rate into the population is Λ and some portion it, $(\varepsilon\Lambda)$, will receive a vaccination at birth where $(0 \le \varepsilon \le 1)$. The natural death rate (any death which is not due to TB) is assumed to be the same for each class and denoted by μ. The mortality due to the TB disease will happen only in the I-class with a rate δ. The efficiency of the BCG vaccine is not complete. Hence, it is assumed that some portion of vaccinated individuals will be susceptible to bacteria with a rate of θ.

Susceptible individuals can be infected with TB through the transmission coefficient β. The treatment rate for the E-class is denoted by α. It is assumed that the untreated portion of the E-class will develop active TB at the rate k. If treatment is administered for the I-class with a rate r, then some of them will complete their treatment correctly at a rate $(1-p)r$ for $(0 \le p \le 1)$. The recovered individuals are moved to the L-class because treatment cannot eradicate the TB bacteria from the body of the patients. Hence, recovered and low-risk latently infected individuals are classified into a single class of low-risk latent individuals. It is assumed that there is no permanent immunity to tuberculosis hence some of the recovered (low-risk latent) individuals can lose their immunity and become high-risk-latently infected, with the relapse rate σ. We further assume that all parameters to be used in this model are nonnegative.

Given these assumptions, we have the following flow diagram, which describes the interaction between classes (Figure 1).

Based on our definitions, assumptions, and interrelations between the variables, the system of ODE that describes the dynamics of TB is formulated as follows,

$$\begin{cases} \dfrac{dS}{dt} &= (1-\varepsilon)\Lambda + \theta V - \beta SI - \mu S, \\ \dfrac{dV}{dt} &= \varepsilon\Lambda - (\theta+\mu)V, \\ \dfrac{dE}{dt} &= \beta SI + pr\mathrm{I} + \sigma L - (k+\alpha+\mu)\mathrm{E}, \\ \dfrac{dI}{dt} &= kE - (\mu+r+\delta)\mathrm{I}, \\ \dfrac{dL}{dt} &= (1-p)r\mathrm{I} + \alpha\,\mathrm{E} - (\mu+\sigma)L, \\ N(t) &= S(t)+V(t)+E(t)+I(t)+L(t). \end{cases} \tag{1}$$

2.2. Basic Properties

2.2.1. Positivity of Solutions.

Theorem 1. *Let the initial data S_0, V_0, E_0, I_0 and L_0 be nonnegative. Then the solution set $t > 0$.*

Proof. Take the second equation of the model (1)

$$\frac{dV(t)}{dt} = \varepsilon\Lambda - (\theta+\mu)V(t). \tag{2}$$

For simplicity let us write $\theta + \mu = \varphi$ and $\varepsilon\Lambda = \lambda$. Then,

$$\frac{dV(t)}{dt} + \varphi V(t) = \lambda. \tag{3}$$

Multiplying both sides of (3) by $\exp(\varphi t)$ gives

$$\frac{dV(t)}{dt}\exp(\varphi t) + \varphi V(t)\exp(\varphi t) = \lambda\exp(\varphi t). \tag{4}$$

By the product rule of the derivative we have

$$\frac{dV(t)}{dt}\exp(\varphi t) + \varphi V(t)\exp(\varphi t) = \frac{d}{dt}[V(t)\exp(\varphi t)]. \tag{5}$$

Hence from (4), we have

$$\frac{d}{dt}[V(t)\exp(\varphi t)] = \lambda\exp(\varphi t). \tag{6}$$

Integrating both sides of (6) gives

$$V(t) = V(0)\exp(-\varphi t) + \frac{\lambda}{\varphi}(1-\exp(-\varphi t)) \ge 0. \tag{7}$$

Similarly taking the first equation of (1) gives

$$\frac{dS(t)}{dt} = (1-\varepsilon)\Lambda + \theta V(t) - (\beta I(t) - \mu)S(t). \tag{8}$$

By letting $(1-\varepsilon)\Lambda = \phi$ and $(\beta I(t) - \mu) = H(t)$, we have

$$\frac{dS(t)}{dt} + H(t)S(t) = \phi + \theta V(t). \tag{9}$$

Multiply both sides of (9) by $\exp\left\{\int_0^t H(\tau)d\tau\right\}$ gives

$$\begin{aligned} &\frac{dS(t)}{dt}\exp\left\{\int_0^t H(\tau)d\tau\right\} + H(t)S(t)\exp\left\{\int_0^t H(\tau)d\tau\right\} \\ &\quad = \phi\exp\left\{\int_0^t H(\tau)d\tau\right\} + \theta V(t)\exp\left\{\int_0^t H(\tau)d\tau\right\}, \end{aligned} \tag{10}$$

By the product rule of the derivative, we have

$$\frac{dS(t)}{dt}\exp\left\{\int_0^t H(\tau)d\tau\right\} + H(t)S(t)\exp\left\{\int_0^t H(\tau)d\tau\right\} = \frac{d}{dt}\left[S(t)\exp\left\{\int_0^t H(\tau)d\tau\right\}\right]. \tag{11}$$

Hence

$$\frac{d}{dt}\left[S(t)\exp\left\{\int_0^t H(\tau)d\tau\right\}\right] = \phi\exp\left\{\int_0^t H(\tau)d\tau\right\} + \theta V(t)\exp\left\{\int_0^t H(\tau)d\tau\right\}. \tag{12}$$

Integrating both sides of (12) gives

$$S(t)\exp\left\{\int_0^t H(\tau)d\tau\right\} - S_0 = \phi\int_0^t \exp\left\{\int_0^\tau H(u)du\right\} + \int_0^t \theta V(u)\exp\left\{\int_0^\tau H(u)du\right\}. \tag{13}$$

Then

$$\begin{aligned} S(t) = S_0\exp\left\{-\int_0^t H(\tau)d\tau\right\} &+ \left[\phi\int_0^t \exp\left\{\int_0^\tau H(u)du\right\}\right] \\ &\cdot \left[\exp\left\{-\int_0^t H(\tau)d\tau\right\}\right] \\ &+ \left[\int_0^t \theta V(u)\exp\left\{\int_0^\tau H(u)du\right\}\right] \\ &\cdot \left[\int_0^t \theta V(u)\exp\left\{\int_0^\tau H(u)du\right\}\right] \geq 0. \end{aligned} \tag{14}$$

Similarly, we can show that $E(t), I(t)$, and $L(t)$ are nonnegative. □

Remark. Note that, in particular, from equation (13) it follows that

$$\lim_{t\to\infty} V(t) = \frac{\varepsilon\Lambda}{\theta+\mu}. \tag{15}$$

2.2.2. Invariant Regions

Theorem 2. *With the nonnegative initial conditions, the feasible region of the model is defined by*

$$\Omega = \left\{(S(t), V(t), E(t), I(t), L(t)) \in \mathbb{R}_+^{\,5} | S(t) + V(t) + E(t) + I(t) + L(t) \leq \frac{\Lambda}{\mu}\right\}. \tag{16}$$

Proof. The change of total population size is

$$\frac{dN(t)}{dt} = \frac{dS(t)}{dt} + \frac{dV(t)}{dt} + \frac{dE(t)}{dt} + \frac{dI(t)}{dt} + \frac{dL(t)}{dt} = \Lambda - \mu N(t) - \delta \mathrm{I}(t) \leq \Lambda - \mu N(t). \tag{17}$$

The inequality (17) implies

$$N(t) \leq \frac{\Lambda}{\mu} - N_0\exp(-\mu t). \tag{18}$$

Thus for every $t > 0$, as $t \to \infty$, $N(t) \leq \frac{\Lambda}{\mu}$.

Hence an invariant region for this model is

$$\Omega = \left\{(S(t), V(t), E(t), I(t), L(t)) \in \mathbb{R}_+^{\,5} | S(t) + V(t) + E(t) + I(t) + L(t) \leq \frac{\Lambda}{\mu}\right\}. \tag{19}$$

□

3. Model Analysis

3.1. Disease-Free Equilibrium Point and the Basic Reproduction Number. The disease-free equilibrium point of the model (1) is given by:

$$P_0^* = (S_0^*, V_0^*, 0, 0, 0), \tag{20}$$

where $S_0^* = \Lambda/\mu(\theta + \mu(1-\varepsilon))/(\theta+\mu)$, and $V_0^* = \varepsilon\Lambda/(\theta+\mu)$.

The basic reproduction number ($\mathscr{R}_0$) is the expected average number of new TB infections caused by a single infected individual when in contact with a completely susceptible population. We obtained $\mathscr{R}_0$ by using the next-generation matrix method given in [17], this amounts to calculating the two matrices M and F, where M is the rate of transfer of individuals into and out of the infected classes and F is the rate of new infections in the compartment. Hence, by the equations we obtain,

$$F = \begin{pmatrix} 0 & \beta\Lambda\left(\frac{1}{\mu} - \frac{\varepsilon}{\theta+\mu}\right) & 0 \\ 0 & 0 & 0 \\ 0 & 0 & 0 \end{pmatrix}, \tag{21}$$

$$M = \begin{pmatrix} k+\alpha+\mu & -pr & -\sigma \\ -k & r+\delta+\mu & 0 \\ -\alpha & (-1+p)r & \mu+\sigma \end{pmatrix}. \tag{22}$$

Then $\mathscr{R}_0$ is the dominant eigenvalue of the matrix FM^{-1}.

Thus we have $\mathscr{R}_0 = (k\beta\Lambda[\theta+\mu(1-\varepsilon)](\mu+\sigma))/(\mu(\theta+\mu)[\mu(r+\delta+\mu)(\alpha+\mu+\sigma) + k\{r\mu(1-p) + (\delta+\mu)(\mu+\sigma)\}])$.

The following number, $\mathscr{R}_g$, serves as an indicator for global stability of the disease-free equilibrium point:

$$\mathscr{R}_g = \frac{k\beta\Lambda[\theta+\mu(1-\varepsilon)+\eta]}{\mu(\theta+\mu)[\mu_1\mu_2 - kpr]}, \tag{23}$$

with $\mu_1 = \alpha+\mu+k$, $\mu_2 = r+\delta+\mu$, and $\eta = (\mu\sigma/k\beta\Lambda)[\alpha\mu_1 + (1-p)rk]$.

Note that since $p \leq 1$ and $\mu > 0$, we are guaranteed that $\mu_1\mu_2 - kpr > 0$.

Theorem 3. *For model (1), the disease-free equilibrium point P_0^* is globally asymptotically stable if $\mathscr{R}_g < 1$.*

Proof. We follow a methodology similarly as in the stability analysis of [18, 19].

For $\mathscr{R}_g < 1$ we have

$$\frac{k\beta\Lambda[\theta+\mu(1-\varepsilon)+\eta]}{\mu(\theta+\mu)} - [\mu_1\mu_2 - kpr] < 0. \tag{24}$$

This can be written as

$$\frac{k\beta\Lambda[\theta+\mu(1-\varepsilon)]}{\mu(\theta+\mu)} + \frac{k\beta\Lambda\eta}{\mu(\theta+\mu)} - [\mu_1\mu_2 - kpr] < 0. \tag{25}$$

By the Archimedean property of $\mathbb{R}$, there exists $\gamma_0 > 0$, for which

$$\frac{k\beta\Lambda[\theta+\mu(1-\varepsilon)]}{\mu(\theta+\mu)} + \gamma_0 k\beta + \frac{k\beta\Lambda\eta}{\mu(\theta+\mu)} - [\mu_1\mu_2 - kpr] < 0. \tag{26}$$

Also, we can find a number γ_1, with $0 < \gamma_1 < \mu$, and such that

$$\frac{k\beta\Lambda[\theta+\mu(1-\varepsilon)]}{\mu(\theta+\mu)} + \gamma_0 k\beta + \frac{k\beta\Lambda\eta}{\mu(\theta+\mu)}\frac{\sigma+\gamma_1}{\gamma_1} - [\mu_1\mu_2 - kpr] < 0. \tag{27}$$

We require an upper bound for $S(t)$. From Remark (15) it follows that there exists t_0 such that $|V(t) - \varepsilon\Lambda/(\theta+\mu)| < \gamma_0$ whenever $t < t_0$. Without loss of generality, we can assume that $|V(t) - \varepsilon\Lambda/(\theta+\mu)| < \gamma_0$ whenever $t > 0$.

The latter inequality implies that $\varepsilon\Lambda/(\theta+\mu) - \gamma_0 < V(t)$ and consequently, that $-V(t) < -\varepsilon\Lambda/(\theta+\mu) + \gamma_0$. Also, we have $N(t) \le \Lambda/\mu$.

Thus for every $t > 0$,

$$S(t) \le N(t) - V(t) < \frac{\Lambda}{\mu} - \frac{\varepsilon\Lambda}{\theta+\mu} + \gamma_0 = \frac{\Lambda}{\mu}\frac{\theta+\mu(1-\varepsilon)}{(\theta+\mu)} + \gamma_0. \tag{28}$$

Now taking $\gamma_2 = \gamma_1/2$, we introduce two constants C_0 and C_1 as follows:

$$C_0 = \frac{\mu_2}{k} - \frac{\alpha(\sigma+\gamma_1)}{k(\mu+\sigma)}, \tag{29}$$

$$C_1 = \frac{\sigma+\gamma_2}{\mu+\sigma}. \tag{30}$$

In particular then, $C_0 > 0$.

Now we define a function:

$$Q(t) = E(t) + C_0 I(t) + C_1 L(t). \tag{31}$$

We prove now that $\dot{Q}(t)$ is negative-definite. Note that we can write

$$\dot{Q}(t) = C_2 E + C_3 I + C_4 L, \tag{32}$$

where $C_2 = C_0 k - \mu_2 + C_1\alpha$, $C_3 = \beta S + pr - C_0\mu_1 + (1-p)rC_1$, and $C_4 = \sigma - C_1(\mu+\sigma)$.

Then $C_4 = -\gamma_2 < 0$.

$$C_2 = -\frac{\alpha(\sigma+\gamma_1)}{(\mu+\sigma)} + \frac{\alpha(\sigma+\gamma_2)}{(\mu+\sigma)} = \frac{\alpha(\gamma_2-\gamma_1)}{(\mu+\sigma)}. \tag{33}$$

Since $\gamma_2 < \gamma_1$, it follows that $C_2 < 0$.

We can write kC_3 as:

$$kC_3 = k(\beta S + pr) - \mu_1\mu_2 + C_5, \tag{34}$$

where

$$\begin{aligned} C_5 &= \frac{\mu_1\alpha(\sigma+\gamma_1) + rk(1-p)(\sigma+\gamma_2)}{\mu+\sigma} \\ &\le \frac{\sigma+\gamma_1}{\mu+\sigma}[\mu_1\alpha + rk(1-p)] \\ &= \frac{(\sigma+\gamma_1)k\beta\Lambda}{\sigma\mu(\mu+\sigma)}\eta. \end{aligned} \tag{35}$$

Noting also the upper bound for $S(t)$, we obtain the following inequality

$$\begin{aligned} kC_3 \le& k\left\{\frac{\Lambda\beta}{\mu(\theta+\mu)}[\theta+\mu(1-\varepsilon)] + \gamma_0\beta + pr\right\} \\ &- \mu_1\mu_2 + \frac{k\Lambda\beta}{\mu(\theta+\mu)}\frac{\sigma+\gamma_1}{\sigma}\eta. \end{aligned} \tag{36}$$

Therefore by the inequality (16), it follows that $kC_3 < 0$. This proves that $\dot{Q}(t)$ is negative-definite. Hence, $Q(t)$ is a Lyapunov function on Ω. Therefore, by LaSalle's invariance principle [20], every solution of model (1), with any initial conditions in Ω, approaches P_0^* as $t \to \infty$, whenever $\mathscr{R}_0 < 1$. □

The results in Theorem 3 implies that for any initial size of the subpopulation of the model, TB can be eliminated from the population when $\mathscr{R}_0 < 1$.

3.2. Existence of the Endemic Equilibrium Point. In this section, we show the existence of an endemic equilibrium point of the model (1). The endemic equilibrium point is the steady-state where the disease keeps alive in the population that is when at least one of the infected classes of the model is nonzero.

Theorem 4. *If $\mathscr{R}_0 > 1$, then the model (1) has a unique positive endemic equilibrium*

$$P^* = (S^*, V^*, E, I^*, L^*) \tag{37}$$

with:

$$S^* = \frac{\Lambda[\theta+\mu(1-\varepsilon)]}{\mathscr{R}_0(\theta+\mu)}, \tag{38}$$

$$V^* = \frac{\varepsilon\Lambda}{\theta+\mu}, \tag{39}$$

$$\mathrm{E}^* = \frac{(r+\delta+\mu)\mu}{k\beta}(\mathscr{R}_0 - 1), \tag{40}$$

$$I^* = \frac{\mu}{\beta}(\mathscr{R}_0 - 1), \tag{41}$$

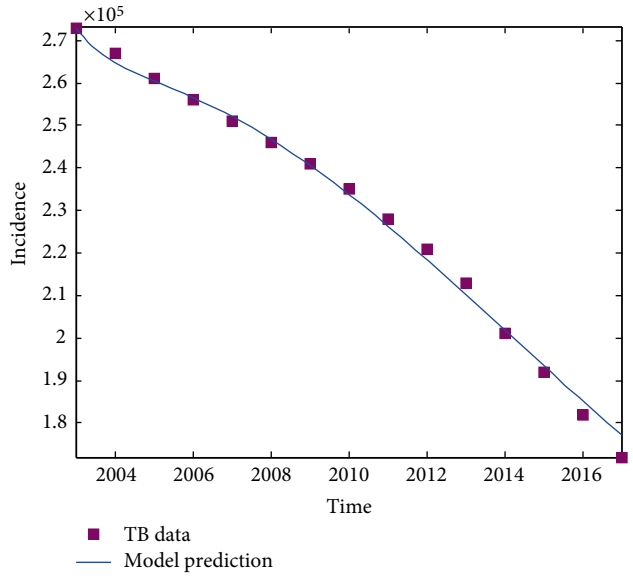

Figure 2: The yearly reported TB incidence data (■) and and the corresponding best fit (solid blue curve) of $kE(t)$.

$$L^* = \frac{\mu(kr(1-p)+\alpha(r+\delta+\mu))(\mathscr{R}_0-1)}{k\beta(\mu+\sigma)}. \quad (42)$$

4. Numerical Simulations

4.1. Estimation of the Model Parameters. In this subsection, we estimate the values of the parameters of the model (1) based on the existing literature and the epidemiological data of Ethiopia in the years between 2003 and 2017. The values of the parameters are summarised in Table 1, and the detailed estimation process of the parameter values is as follows.

(a) According to the World Bank report, [21], the average life expectancy of Ethiopia in the years between 2003 and 2017 is 60.93 years. The natural death rate can be calculated as the inverse of life expectancy [8, 22]. Hence we estimate $\mu = 0.016$.

(b) The upper limit of the total population in the absence of the disease is Λ/μ. Hence it is possible to take Λ as a product of μ and the average population size over the years 2003–2017. Using this formula and the WHO report [23], the average yearly recruitment rate to the population of Ethiopia is 1.4×10^6.

(c) Also, from the WHO report [23], the average TB-induced death rate is approximately $\delta = 0.17$.

(d) From the WHO report, the average BCG vaccination coverage in Ethiopia over the years 2003–2017 is 71.5% [24]. Therefore, we take $\varepsilon = 0.715$.

(e) According to the data obtained from WHO [25], the treatment success rate for TB in Ethiopia is 83.2%. Hence we estimate $1 - p = 0.832$.

(f) On average, the BCG vaccine significantly reduces the risk of TB by 50% [26]. Therefore, $\theta = 0.5$.

(g) The transmission coefficient, progression rate from E-class to I-class, treatment coverage rate of I-class, the relapse rate from L-class to E-class, and treatment rate of E-class are obtained by fitting the yearly TB incidence data obtained from WHO [23] to the model by using fmincon MATLAB routine. Figure 2 shows the graph of TB incidence data obtained (■) and the estimated solid curve. The estimated values are $\beta = 1.646 \times 10^{-7}, \kappa = 0.023, r = 0.546, \sigma = 0.0013$ and $\alpha = 0.153$.

(h) We calculate the initial number of vaccinated children as the product of the average number of newborns and the vaccination coverage, which is $V_0 = 1 \times 10^6$.

(i) The initial fraction for the infectious class $I_0 = 3.73 \times 10^5$ is taken from the TB- prevalence in 2003 reported by the WHO [23].

(j) We estimate the initial value of the E-class and the L-class from the data-fitting process. Thus, the amount of E_0 and L_0 is 16.37% and 30% out of the total population, respectively. This gives $E_0 = 1.19 \times 10^7$ and $L_0 = 2.18 \times 10^7$.

(k) Finally, the initial number of the susceptible class is found from $S_0 = N_0 - (V_0 + E_0 + I_0 + L_0) = 3.75 \times 10^7$.

(l) Consequently, using these estimated parameters values we calculated the average value of $\mathscr{R}_0$ for the year 2003–2017 TB cases in Ethiopia is $\mathscr{R}_0 \approx 2.13$.

Table 1: The parameter values of the model (1).

Parameters	Description	Value	Source
N_0	Initial total population	7.25×10^7	[23]
S_0	The initial number of susceptible individuals	3.75×10^7	Estimated
V_0	The initial number of vaccinated individuals	1×10^6	Estimated
E_0	The initial number of high-risk latent individuals	1.19×10^7	Fitted
I_0	The initial number of infectious individuals	3.73×10^5	[23]
L_0	The initial number of low-risk latent individuals	2.18×10^7	Fitted
Λ	Recruitment rate	1.4×10^6	Estimated
β	The transmission coefficient	1.646×10^{-7}	Fitted
ε	Vaccination coverage rate	0.715	[24]
θ	Loss of protection for vaccination	0.5	[26]
μ	The natural death rate	0.016	Estimated
k	Progression rate from E to I	0.023	Fitted
r	The treatment rate of I	0.546	Fitted
$1 - p$	Successful treatment rate of I	0.832	[25]
α	Treatment rate of E	0.153	Fitted
δ	TB induced death rate	0.17	[23]
σ	The relapse rate	0.0013	Fitted

4.2. Sensitivity Analysis of the Basic Reproduction Number. To determine the best strategy for reducing human mortality and morbidity due to TB, it is crucial to know the relative

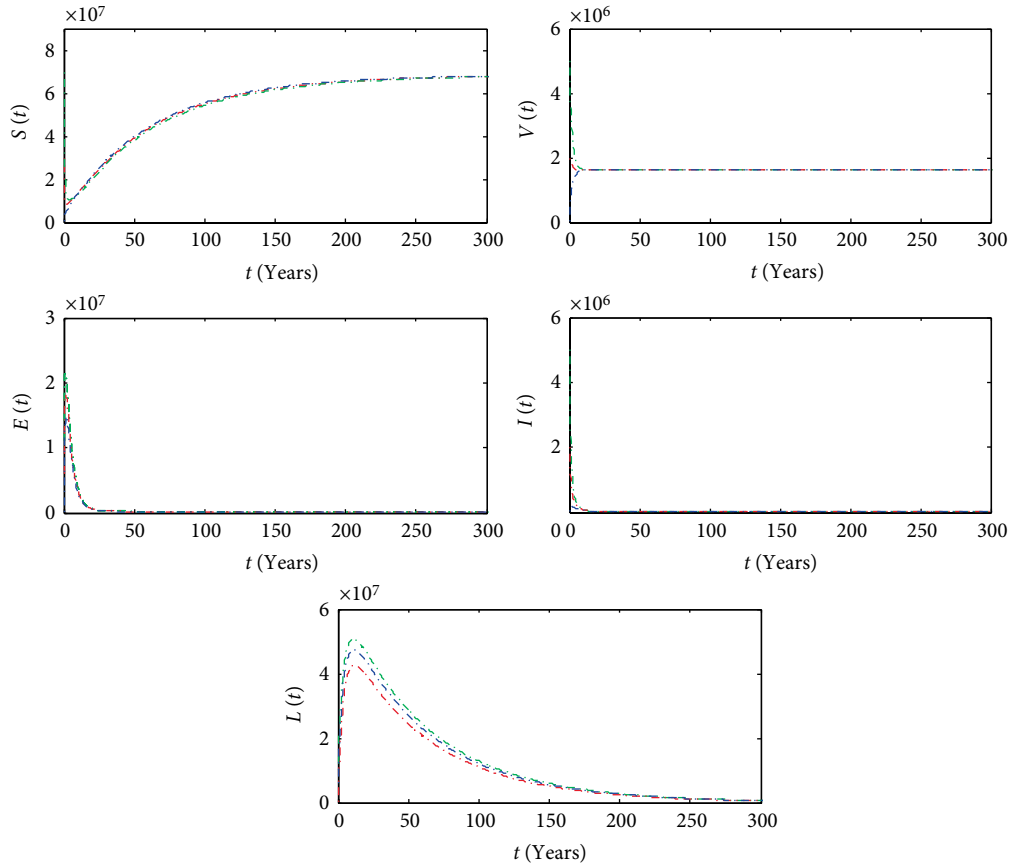

FIGURE 3: The plot shows for different initial values of (S, V, E, I, L), the solution of the model converges to the disease-free equilibrium point $P_0^* = \left(6.84 \times 10^7, 1.61 \times 10^6, 0, 0, 0\right)$ for $\mathscr{R}_g = 0.65$.

TABLE 2: Sensitivity indices of $\mathscr{R}_0$.

Parameters		Sensitivity index of $\mathscr{R}_0$	Corresponding % changes
β	The transmission coefficient	+1	1%
α	Treatment rate of E	−0.801543	+1.25%
r	The treatment rate of I	−0.742021	+1.35%
ε	Vaccination coverage rate	−0.0226732	+44.1%
p	Treatment failure rate	+0.0219702	+45.5%

importance of the different factors responsible for its transmission and prevalence. Sensitivity analysis using the normalized forward sensitivity index is used to determine the relative importance of various parameters accountable for the disease transmission [27]. The basic reproduction number is the most significant threshold in studying the dynamics of infectious disease [28]. In this section, we calculate the sensitivity indices of $\mathscr{R}_0$ for the model parameters by using the normalized forward sensitivity index.

Definition. The normalized forward sensitivity index of $\mathscr{R}_0$ which is differentiable with respect to a given parameter π, is defined by

$$\Gamma_\tau^{\mathscr{R}_0} = \frac{\partial \mathscr{R}_0}{\partial \pi} \times \frac{\pi}{\mathscr{R}_0}. \tag{43}$$

Using this formula, we calculate the sensitivity indices of $\mathscr{R}_0$ with respect to $\beta, \alpha, r, \varepsilon$, and p. The values of $\Gamma_\beta^{\mathscr{R}_0}$ and $\Gamma_p^{\mathscr{R}_0}$ are positive. This tells us, the total number of infected people can be decreased by reducing the contact rate of active TB infected individuals and the treatment failure rate. On the other hand, $\Gamma_\alpha^{\mathscr{R}_0}$, $\Gamma_r^{\mathscr{R}_0}$, and $\Gamma_\varepsilon^{\mathscr{R}_0}$ are negative. This means that TB infection can be controlled by increasing the treatment rate of active and latent TB infected individuals, and vaccination coverage rate. The values of the sensitivity indices for $\mathscr{R}_0$ are summarized in Table 2.

The most sensitive parameter for $\mathscr{R}_0$ is the transmission coefficient β. The next essential parameters are the treatment rates of latent and active TB patients. Table 2 shows that to have 1% decrease in the value of $\mathscr{R}_0$, it is necessary to decrease the amount of β and p to 1%, and 45.5%

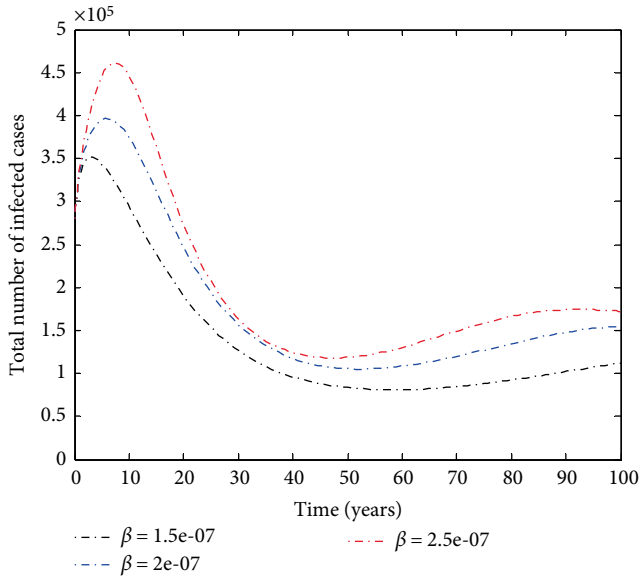

FIGURE 4: The plot shows the effect of transmission coefficient on the total number of infected class.

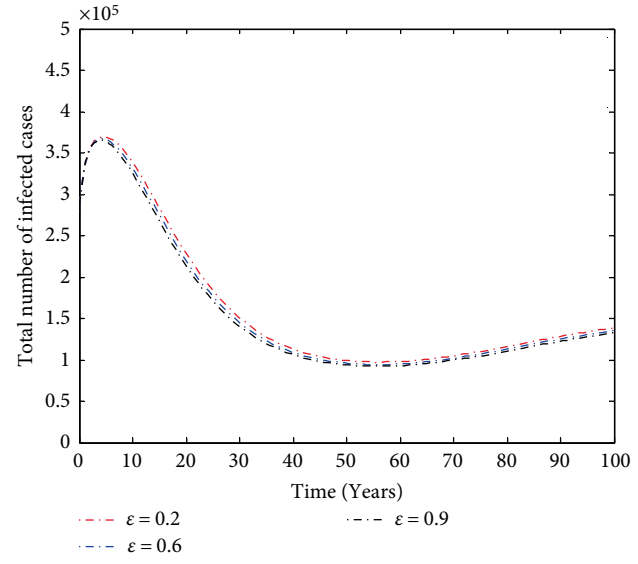

FIGURE 5: The effect of vaccination coverage on the number of infected class.

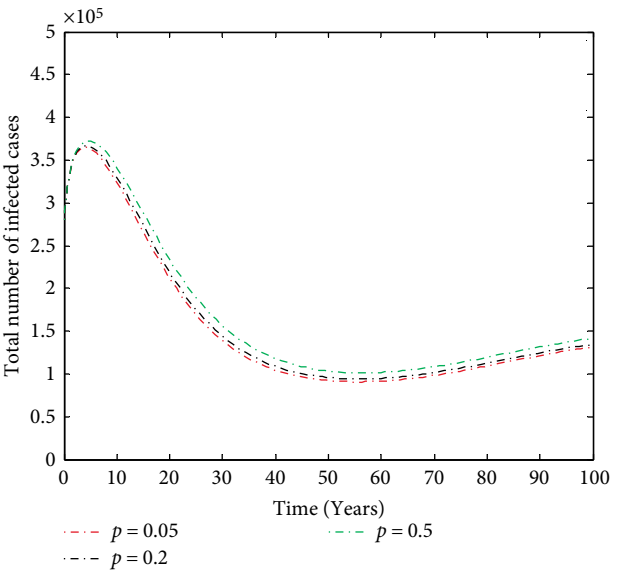

FIGURE 6: The effect of treatment failure rate on the number of infected class.

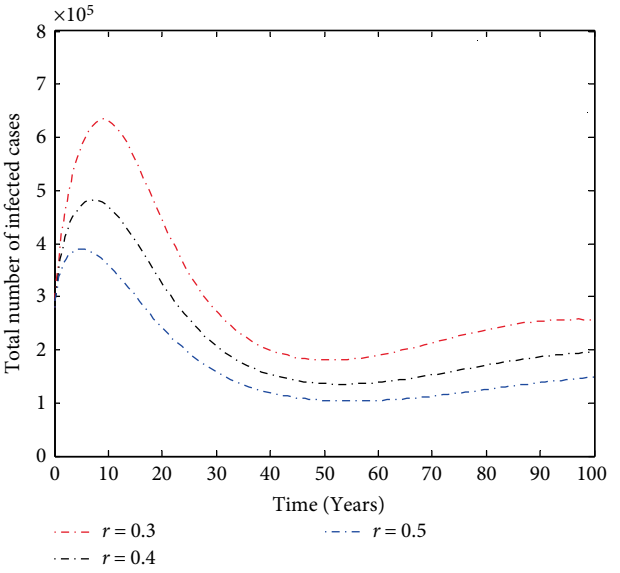

FIGURE 7: The effect of treatment coverage on the number of infected class.

respectively. While to have 1% decrease in the value of $\mathscr{R}_0$ it is necessary to increase the amount of ε, r, and α to 44.1, 1.35, and 1.25% respectively.

4.3. Numerical Simulations. In this subsection, the results of the model are simulated using ODE 45 solvers code in MATLAB programming language. The effect of epidemiological parameters on the number of active TB patients is simulated, and their impact is determined. The results of numerical simulations are displayed graphically.

As shown in Figure 3, for $\mathscr{R}_g < 1$, for different initial conditions the solution curve of the model converges to the disease-free equilibrium point P_0^*, this indicates that P_0^* is globally asymptotically stable for $\mathscr{R}_g < 1$ and this agrees with Theorem 3 (Figure 4).

Figures 5–8 show the effect of different epidemiological parameters on the number of the infected population. It is found that decreasing transmission coefficient (the contact between susceptible class and active TB patients) and minimizing the failure rate of treatment is essential to reduce the number of infected TB patient population. Also, increasing the treatment and vaccination coverage is vital to decrease the amount of infected TB patient population.

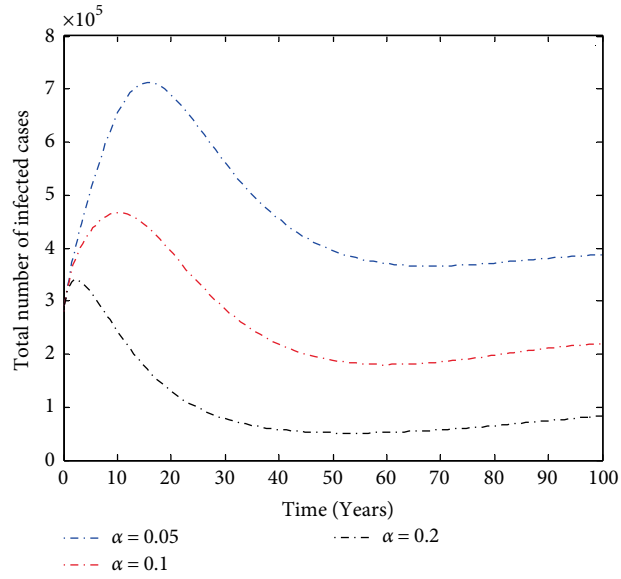

FIGURE 8: The effect of treatment coverage of high-risk latent class on the number of infected class.

5. Conclusion

In this research, we studied a tuberculosis transmission dynamics model with vaccination and treatment for both high-risk latent and active TB infected classes. The reproduction number is calculated and the equilibrium points are described. We showed that the disease-free equilibrium point P_0^* is globally asymptotically stable when $\mathscr{R}_g < 1$, so that the disease dies out. Finally, we showed that an increase in the treatment and vaccination coverage gives rise to a decrease in the number of infected TB patient population.

The parameter values of the model are obtained from the existing literature and by fitting the yearly reported TB incidence cases in Ethiopia. We estimate that the basic reproduction number for TB transmission in Ethiopia is $\mathscr{R}_0 \approx 2.13$. The implication of this is that TB is still endemic in the country, and more emphasis should be given for the prevention of TB transmission. Using sensitivity analysis, we found that the most influential parameter is the transmission coefficient, followed by the treatment rate of latent TB and active TB infective individuals. Therefore, we propose that the effective strategy to eliminate the TB infection from Ethiopia is reducing the transmission coefficient. This will be done by increasing the isolation of infectious people. The second important strategy is to increase the treatment coverage for latent and active TB infectious individuals with proper follow up so that the failure of treatment cases decreases.

Data Availability

No data were used to support this study.

Conflicts of Interest

The authors declare that they have no conflicts of interest.

References

[1] World Health Organization, "Tuberculosis fact sheet N°104" 2012," http://www.who.int/mediacentre/factsheets/fs104/en/, June, 3, 2019.

[2] World Health Organization, *Implementing the WHO Stop TB Strategy: a handbook for national tuberculosis control programmes*, WHO, Geneva, 2008.

[3] A. Roy, M. Eisenhut, R. J. Harris et al., "Effect of BCG vaccination against Mycobacterium tuberculosis infection in children: Systematic review and meta-analysis," *BMJ*, vol. 349, p. g4643, 2014.

[4] Centers for Disease Control and Prevention, ""TB Elimination – BCG vaccine", National Center for HIV/AIDS, Viral Hepatitis, STD, and TB Prevention, Division of Tuberculosis Elimination, 2011," http://www.cdc.gov/tb/publications/factsheets/prevention/bcg.pdf, June, 3, 2019.

[5] World Health Organization, "Global tuberculosis report 2018," http://www.who.int/iris/handle/10665/274453, June 3, 2019.

[6] Centers for Disease Control and Prevention (CDC), "Travelers' Health Ethiopia", 2018, https://www.cdc.gov/globalhealth/countries/ethiopia/pdf/Ethiopia_Factsheet-p.pdf, June, 5, 2019.

[7] H. Waaler, A. Geser, and S. Andersen, "The use of mathematical models in the study of the epidemiology of tuberculosis," *American Journal of Public Health*, vol. 52, no. 6, pp. 1002–1013, 1962.

[8] P. Witbooi, S. Vyambwera, and M., "A model of population dynamics of TB in a prison system and application to South Africa," *BMC Research Notes*, vol. 10, no. 1, pp. 1–8, 2017.

[9] A. Ssematimba, J. Y. T. Mugisha, and L. S. Luboobi, "Mathematical models for the dynamics of tuberculosis in density-dependent populations: the case of internally displaced peoples' camps (IDPCs) in Uganda," *Journal of Mathematics and Statistics*, vol. 1, no. 3, pp. 217–224, 2005.

[10] Z.-W. Jia, G.-Y. Tang, Z. Jin et al., "Modeling the impact of immigration on the epidemiology of tuberculosis," *Theoretical Population Biology*, vol. 73, no. 3, pp. 437–448, 2008.

[11] S. Athithan and M. Ghosh, "Mathematical modelling of TB with the effects of case detection and treatment," *International Journal of Dynamics and Control*, vol. 1, no. 3, pp. 223–230, 2013.

[12] I. M. Wangari, J. Trauer, and L. Stone, "Modelling heterogeneity in host susceptibility to tuberculosis and its effect on public health interventions," *PLoS One*, vol. 13, no. 11, p. e0206603, 2018.

[13] Y. Zhao, L. Mingtao, and Y. Sanling, "Analysis of transmission and control of tuberculosis in Mainland China, 2005–2016, based on the age-structure mathematical model," *International Journal of Environmental Research and Public Health*, vol. 14, no. 10, p. 1192, 2017.

[14] S. Choi and E. Jung, "Optimal tuberculosis prevention and control strategy from a mathematical model based on real data," *Bulletin of Mathematical Biology*, vol. 76, no. 7, pp. 1566–1589, 2014.

[15] D. P. Moualeu, M. Weiser, R. Ehrig, and P. Deuflhard, "Optimal control for a tuberculosis model with undetected cases in Cameroon," *Communications in Nonlinear Science and Numerical Simulation*, vol. 20, no. 3, pp. 986–1003, 2015.

[16] S. Kim, A. A. de los Reyes, and E. Jung, "Mathematical model and intervention strategies for mitigating tuberculosis in the Philippines," *Journal of Theoretical Biology*, vol. 443, pp. 100–112, 2018.

[17] H. M. Yang, "The basic reproduction number obtained from Jacobian and next generation matrices – A case study of dengue transmission modelling," *Biosystems*, vol. 126, pp. 52–75, 2014.

[18] P. J. Witbooi, "Stability of a stochastic model of an SIR epidemic with vaccination," *Acta Biotheoretica*, vol. 65, no. 2, pp. 151–165, 2017.

[19] P. J. Witbooi, "An SEIRS epidemic model with stochastic transmission," *Advances in Difference Equations*, vol. 2017, Article ID 109, 2017.

[20] J. P. LaSalle, *The Stability of Dynamical Systems*, Hamilton Press, New Jersey, NJ, USA, 3rd edition, 2002.

[21] World Bank, "Life expectancy at Birth 2018," https://www.google.com/url?sa=t&sou rce=web&rct=j&url=https://api.worldbank.org/ v2/en/indicator/SP.DYN.LE00.IN%3Fdownloadf ormat%3Dexcel&ved=2ahUKEwjOveTDtMLgAhU2SBUIHdv4DFkQFjABegQIBxA B&usg=AOvVaw18U96SZo CkZGQq8dOT8Ehz, July 2, 2019.

[22] S. Ullah, M. Khan, A. M. Farooq, and T. Gul, "Modeling and analysis of Tuberculosis (TB) in Khyber Pakhtunkhwa, Pakistan," *Mathematics and Computers in Simulation*, vol. 165, pp. 181–199, 2019.

[23] World Health Organization, "WHO TB burden estimates 2018," https://www.who.int/tb/country/data/download/en/, June 4, 2019.

[24] World Health Organization, "WHO vaccine-preventable diseases: monitoring system. 2019 global summary 2019," https://apps.who.int/immunization_monitoring/globalsummary/estimates?c=ETH, July 2, 2019.

[25] World Health Organization, "Treatment success data by country 2018," http://apps.who.int/gho/data/node.main.602?lang=en, June 5, 2019.

[26] G. A. Colditz, "Efficacy of BCG vaccine in the prevention of tuberculosis," *JAMA*, vol. 271, no. 9, pp. 698–702, 1994.

[27] Chitnis N. Mac, J. Hyman, and J. M. Cushing, "Determining important parameters in the spread of malaria through the sensitivity analysis of a mathematical model," *Bulletin of Mathematical Biology*, vol. 70, no. 5, pp. 1272–1296, 2008.

[28] P. van den Driessche, "Reproduction numbers of infectious disease models," *Infectious Disease Modelling*, vol. 2, no. 3, pp. 288–303, 2017.